Supplementary Material (ESI) for New Journal of Chemistry

Guest induced gate-opening of a Zeolite Imidazolate Framework

Sonia Aguado, Gérard Bergeret, Marc Pera Titus, Virginie Moizan, Carlos Nieto-Draghi, Nicolas Bats, and David Farrusseng*

Supporting Information

1.- Gas sorption analysis

CO_2 adsorption/desorption isotherms at different temperatures were measured on a BELSORP-HP. The samples were outgassed under vacuum (~ 10-4 mbar) at 473 K for 12 h before beginning the measurements.

2.- Isotherm modelling

Eq. 1 includes eight parameters, four accounting for energy heterogeneity and four for the sorbate/sorbent interaction. The original Eq. 1 can be simplified so that the different sets of (m, k) parameters can be fitted individually. Eq. 1 has been fitted first to both adsorption and desorption isotherm data in order to provide accurate estimates of gate-opening free energies of ZIF-7 upon CO_2 adsorption. Thermodynamic expressions and fitted values are reported in the Supporting Information. (P~Pc=74 bar for CO_2). For ELM-11, the adsorption data were taken from Kanoh *et al.* For MIL-53(Al), adsorption measurements were carried out.

$$-\frac{\Psi}{RT}=\int_{\theta}^{1}\left[-Ln(\Pi)\right]\delta\theta=\frac{G^{\circ}}{1+\left.\frac{\lambda_1\lambda_2}{\lambda_1+\lambda_2}\right|_A+\left.\frac{\lambda_3\lambda_4}{\lambda_3+\lambda_4}\right|_B} \qquad (1)$$

3.- X-ray diffraction (XRD)

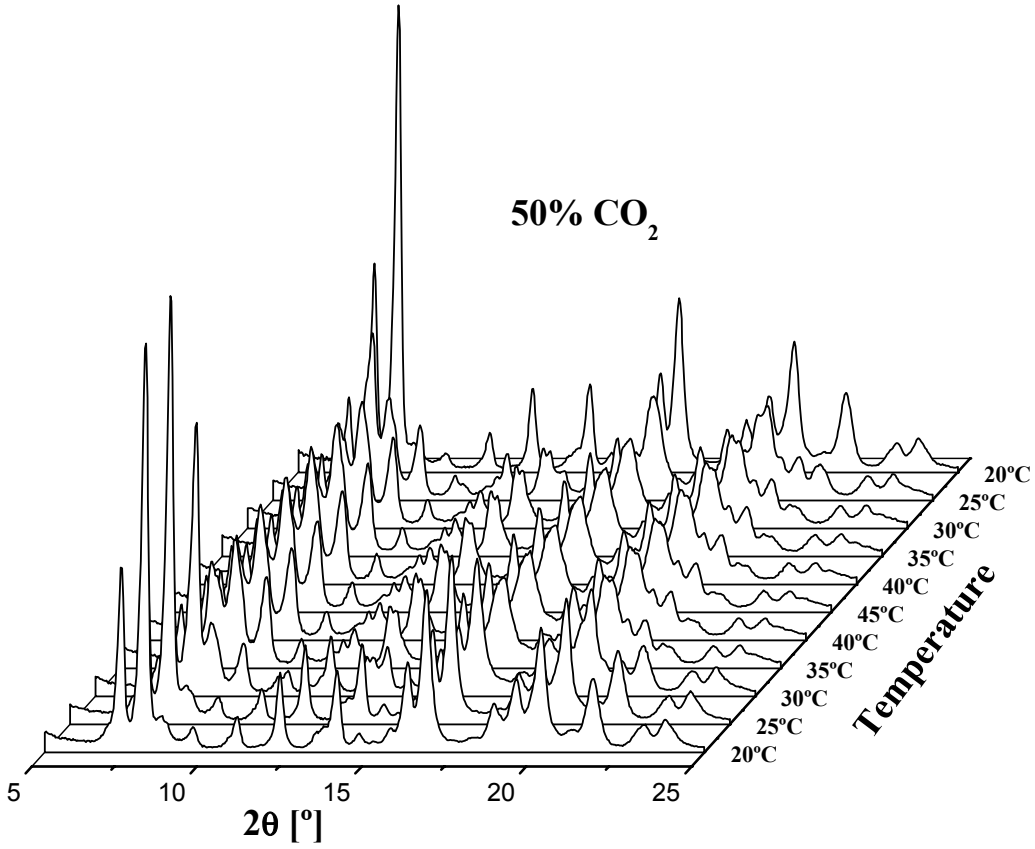

Figure S1: As a function of the temperature, 50% of CO_2

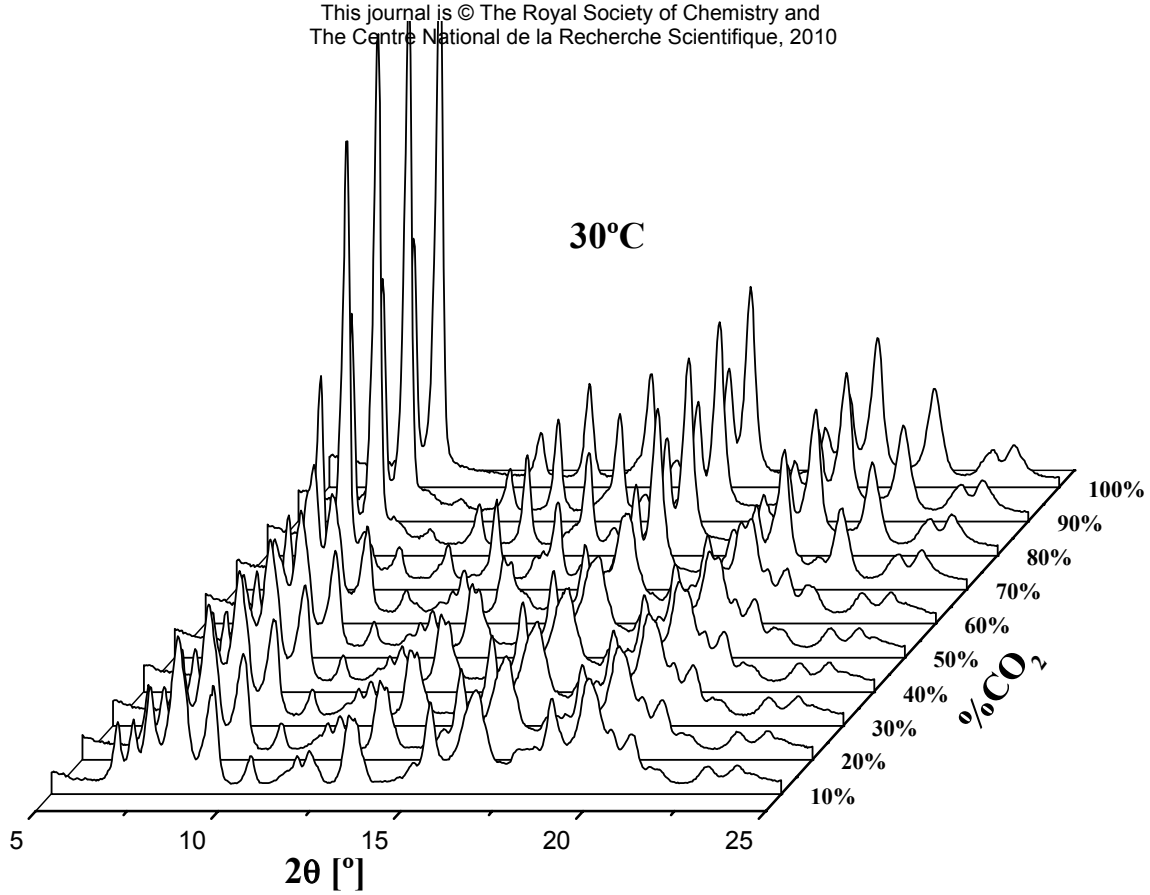

Figure S2: As a function of the CO_2 molar ratio, 303 K, adsorption.

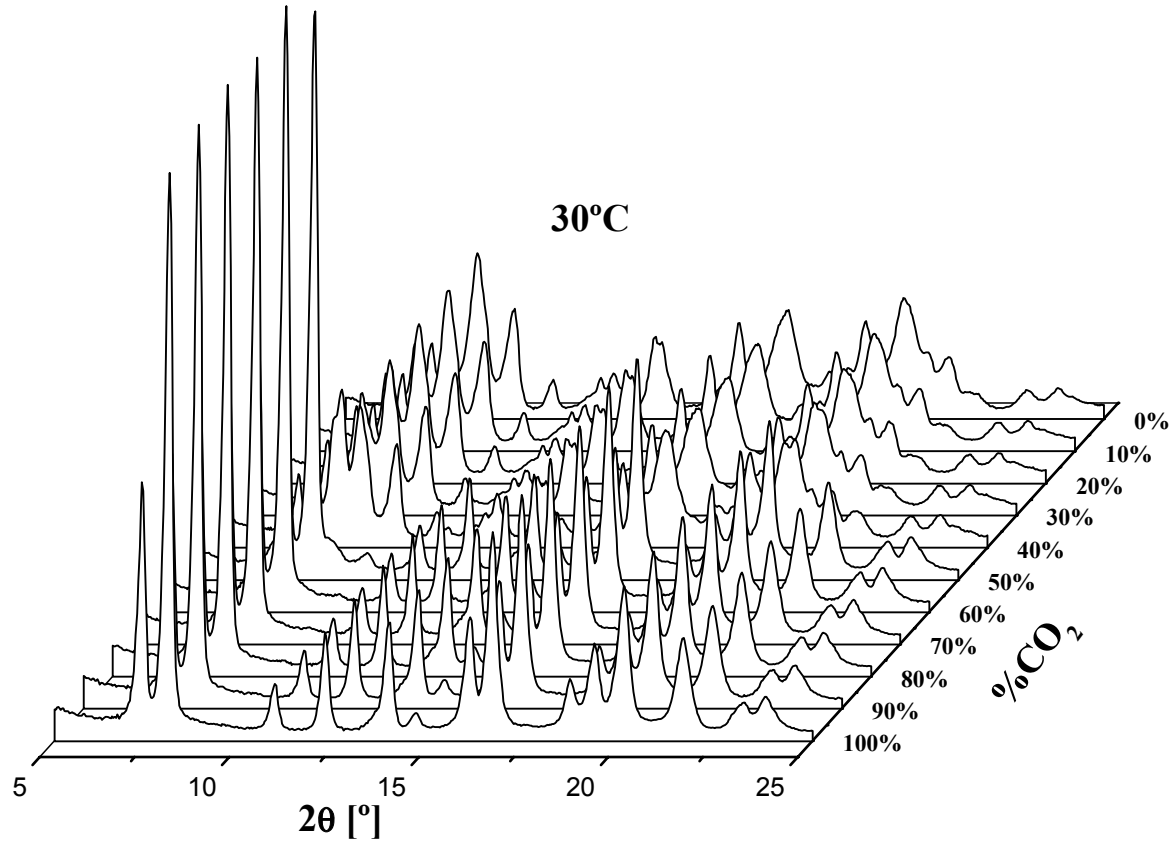

Figure S3: As a function of the CO_2 molar ratio, 303 K, desorption.

4.- Simulation methods

GCMC (Grand Canonical Monte Carlo) simulations combined with a bias scheme [1] for the insertion of the centre of mass of the guest molecules were performed to calculate the adsorption isotherms with the GIBBS code v.8.3.[2] A bias scheme was used for enhancing the acceptance rate of insertions. The selected probabilities for the different moves were generally set to 0.35 for rigid-body translations, 0.10 for rigid-body rotation and 0.55 for insertions or deletions. Systems were allowed to equilibrate for at least one million MC steps followed by production runs of at least 10 million MC steps. The atomic positions of the solid were frozen during the simulations using the open (lp) structure.[3] This allowed the construction of a guest-host interaction energy grid prior to the MC simulations. All simulations were performed in a simulation box incorporating 1×2×3 unit cells for **ZIF-7**, in the orthorhombic equivalent of the triclinic (lp) structure. LJ interactions and real space electrostatic contributions were calculated using a cutoff radius of ~17 Å. No Lennard-Jones tail corrections were considered,[4] however, standard long range electrostatic interactions were calculated using the Ewald methodology with 10 vectors on the reciprocal space and a screening factor nα of 2.5. Crystallographic positions of the ZIF-7 materials were taken from the data available in the Cambridge Structural Data Base.[5] Pores in ZIF-7 for the open structure are fully accessible by CO_2 molecules and consequently no artificial blocking of cavities are required.

In order to determine the fugacities corresponding to the different pressure conditions, simulations in the isobaric-isothermal (NPT) ensemble combined with the particle insertion method were performed.[6] In this case the selected probabilities for MC moves were set to 0.63 for rigid-body translations, 0.35 for rigid-body rotation (only in the case of CO_2, N_2 and CO) and 0.02 for volume changes. Since we have performed adsorption at relative low pressures (below 100 kPa) no correction has been added to our simulations to transform absolute adsorption into excess quantities. In order to consider electrostatic interactions between the solid framework and guest molecules we require the electrostatic potential interaction of ZIF-7. We have assumed that the partial charges on each atom are exactly the same as the one obtained in our previous work for ZIF-11 since both solids have bIM as an organic linker (see Figure S4). Additional details about the different force fields used to describe the adsorbed molecules and DFT calculations can be found ref. [7] and are listed in Table S1.

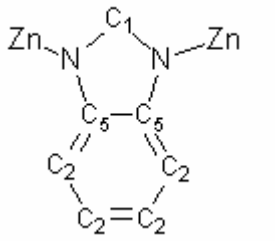

Figure S4: bIm linker of ZIF-7.

Table S1: Non bonded Van der Waals interaction parameters for ZIF-7 materials. See figure S4 for the details of the different types of atoms.

Non–bonded interactions			
Atom type	ε(K)	σ(nm)	q(e)
Zn	43.084	0.2338	1.1
N	23.974	0.3097	-0.465
C1	36.483	0.3259	0.39
C5	36.483	0.3259	0.0
C2	36.483	0.3259	-0.12
H	15.288	0.2440	0.094

Concerning guest molecules, we have used the EPM2 model proposed by Harris and Young [8] to describe CO_2 molecules. This model consists of two different LJ types combined with electrostatic atomic charges. It reproduces accurately the phase equilibrium, critical and transport properties of carbon dioxide. Parameters are listed in Table S2.

Table S2: Guest adsorbed molecules interaction parameters.

CO_2			
Atom type	q(e)	ε(K)	σ(nm)
C	0.6512	28.129	0.2757
O	-0.3256	80.507	0.3033
dC-O(nm)	0.1149		

References

[1] A.D. Mackie, B. Tavitian, A. Boutin et A.H. Fuchs, *Molec. Sim*., **1997**, 19, 1-15.

[2] P. Ungerer, C. Nieto-Draghi, V. Lachet, A. Wender, A. di Lella, A. Boutin, B. Rousseau, A. Fuchs, *Mol. Sim.*, **2007**, 33, 287-304.

[3] X. Huang, J. Zhang and X. Chen, *Chin. Sci. Bull.*, **2003**, 48, 1531-1534.

[4] M. P. Allen, D. J. Tildesley in *Computer Simulation of Liquids*; Oxford University Press: New York, **1989**.

[5] Crystallographic Data Centre http://www.ccdc.cam.ac.uk/

[6] D. Frenkel, B. Smit in *Understanding Molecular Simulation: From Algorithms to Applications*; Academic Press: San Francisco, **2001**.

[7] J. Pérez-Pellitero, A. H., F. Siperstein, G. Pirngruber, C. Nieto-Draghi, G. Chaplais, A. Simon-Masseron, D. Bazer-Bachi, D. Peralta and N. Bats, *Chem. Eur. J.*, **2010**, 16, 1560-1571.

[8] Harris, J.G.; Yung, K.H. J. Phys Chem. **1995**, 99, 12021-12024

5.- Isotherm modelling

Eq. 1 includes 8 parameters, four accounting for energy heterogeneity (m1, m2, m3, m4) and four for the sorbate/sorbent interaction (k1, k2, k3, k4).

$$-\frac{\Psi}{RT}=\int_{\theta}^{1}\left[-Ln(\Pi)\right]\delta\theta=\frac{G^{\circ}}{1+\left.\frac{\lambda_1\lambda_2}{\lambda_1+\lambda_2}\right|_A+\left.\frac{\lambda_3\lambda_4}{\lambda_3+\lambda_4}\right|_B} \tag{1}$$

with Go=-Φ(Po)/RT, λi=kiZmi=(Z/Zi)mi for i=1:4, being Zi=(1/ki)1/mi, being Φ(P°) the surface potential at saturation pressure. The subscripts 'A' and 'B' refer to different phases in the solid.

The energy difference ascribed to the phase transition, ΔG(np→lp), can be then computed as follows:

$$\Delta G\left(np\rightarrow lp\right)=\Delta G_{des-ads}\big|_G+\left[\theta_{des}\left(\Pi_G\right)-\theta_{ads}\left(\Pi_G\right)\right]Ln\left(\Pi_G\right)=$$

$$=\int_{\theta_G}^{1}\left[-Ln\left(\Pi\right)\right]\delta\theta\Big|_{des}-\int_{\theta_G}^{1}\left[-Ln\left(\Pi\right)\right]\delta\theta\Big|_{ads}+\Delta G^{\circ}+\left[\theta_{des}\left(\Pi_G\right)-\theta_{ads}\left(\Pi_G\right)\right]Ln\left(\Pi_G\right)= \tag{2}$$

where the subscript G refers to the gate opening pressure.

In order to obtain statistically significant fittings, we found that the original Eq. 1 can be conveniently simplified to the following expressions accounting, respectively, for CO2 adsorption and desorption.

Adsorption:

$$-\frac{\Psi}{RT}=\int_{\theta}^{1}Z^{-1}\,\delta\theta=\frac{G^{o}_{ads}}{1+\left.\frac{\lambda_1\lambda_2}{\lambda_1+\lambda_2}\right|_A+\left.\frac{\lambda_3\lambda_4}{\lambda_3+\lambda_4}\right|_B}\approx\frac{G^{o}_{ads}}{1+\lambda_1\big|_A+\left.\frac{\lambda_3\lambda_4}{\lambda_3+\lambda_4}\right|_B} \tag{3}$$

Desorption:

$$-\frac{\Psi}{RT}=\int_{\theta}^{1}Z^{-1}\,\delta\theta=\frac{G^{o}_{des}}{1+\left.\frac{\lambda_1\lambda_2}{\lambda_1+\lambda_2}\right|_A+\left.\frac{\lambda_3\lambda_4}{\lambda_3+\lambda_4}\right|_B}\approx\frac{G^{o}_{des}}{1+\left.\frac{\lambda_3\lambda_4}{\lambda_3+\lambda_4}\right|_B} \tag{4}$$

Eqs. 3 and 4 were fitted to the adsorption and desorption data in two/three steps for each relevant zone of the thermodynamic isotherm representation. Using this approach, the different set of (m, k) parameters could be fitted individually. Following table SI-1 collects the fitted values of the relevant parameters in Eqs. 4 and 5. More details about the fitting strategy can be found in ref. [9].

A law of adsorption can be further proposed by relating the integral in Eqs. 3 and 4 with variable Z after numerical integration. Some analytical expressions can be derived at the bounds of the system (see ref. [10] for further details).

References

[9] M. Pera-Titus, M. Savonnet and D. Farrusseng, *J. Phys. Chem. C*, **2010**, 114, 17665-17674.

[10] M. Pera-Titus, *J. Colloid Interface Sci.*, **2010**, 345, 410-416.

5.1- ZIF-7 at 303K

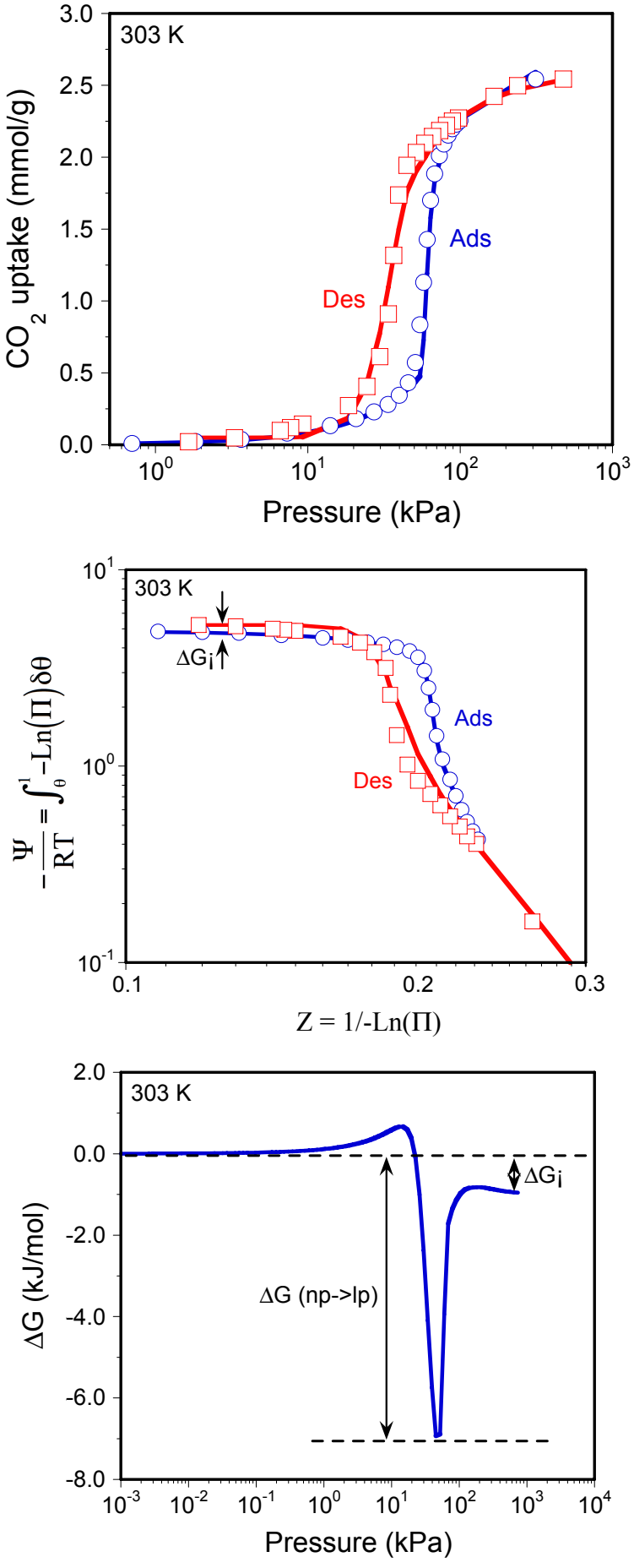

Figure S5: Isotherm modelling for ZIF-7/CO_2 system at 303K; raw isotherm; thermodynamic representation; and free energy changes upon adsorption.

Table S3: Adsorption curve

T (K)	*G°*	*First zone*		*Third zone*		*Fourth zone*	
		m_1	Z_1	m_3	Z_3	m_4	Z_4
273	5.71	-	-	40 ± 9	0.1691 ± 0.0008	10.6 ± 0.9	0.168 ± 0.004
303	4.85	5.4 ± 0.3	0.252 ± 0.004	91 ± 2	0.2065 ± 0.0001	10.8 ± 0.7	0.187 ± 0.002
308	4.70	5.7 ± 0.2	0.262 ± 0.005	73 ± 3	0.2138 ± 0.0002	15.7 ± 0.6	0.203 ± 0.001
323	4.30	5.3 ± 0.1	0.285 ± 0.003	63 ± 2	0.232 ± 0.001	6.3 ± 0.6	0.186 ± 0.007

Table S4: Desorption curve

T (K)	*G°*	*First zone*		*Fourth zone*	
		m_1	Z_1	m_4	Z_4
273	6.01	20 ± 4	0.1572 ± 0.0004	8.7 ± 0.8	0.152 ± 0.002
303	5.24	40 ± 5	0.1855 ± 0.0006	6.3 ± 0.2	0.154 ± 0.002
308	5.10	18 ± 2	0.200 ± 0.002	15 ± 6	0.193 ± 0.002
323	4.61	21 ± 2	0.209 ± 0.001	6.4 ± 0.6	0.180 ± 0.003

Table S5: Phase transition (data in kJ/mol)

T (K)	*ΔG° (kJ/mol)*	*ΔG (des->ads) (kJ/mol)*	*ΔG (np->lp) (kJ/mol)*	P_{peak} *(kPa)*
273	-0.7	-4.7	-3.0	14.8
303	-1.0	-7.0	-4.1	51.8
308	-1.0	-3.8	-2.0	59.2
323	-0.8	-4.8	-4.3	74.0

5.2- MIL-53 at 303K

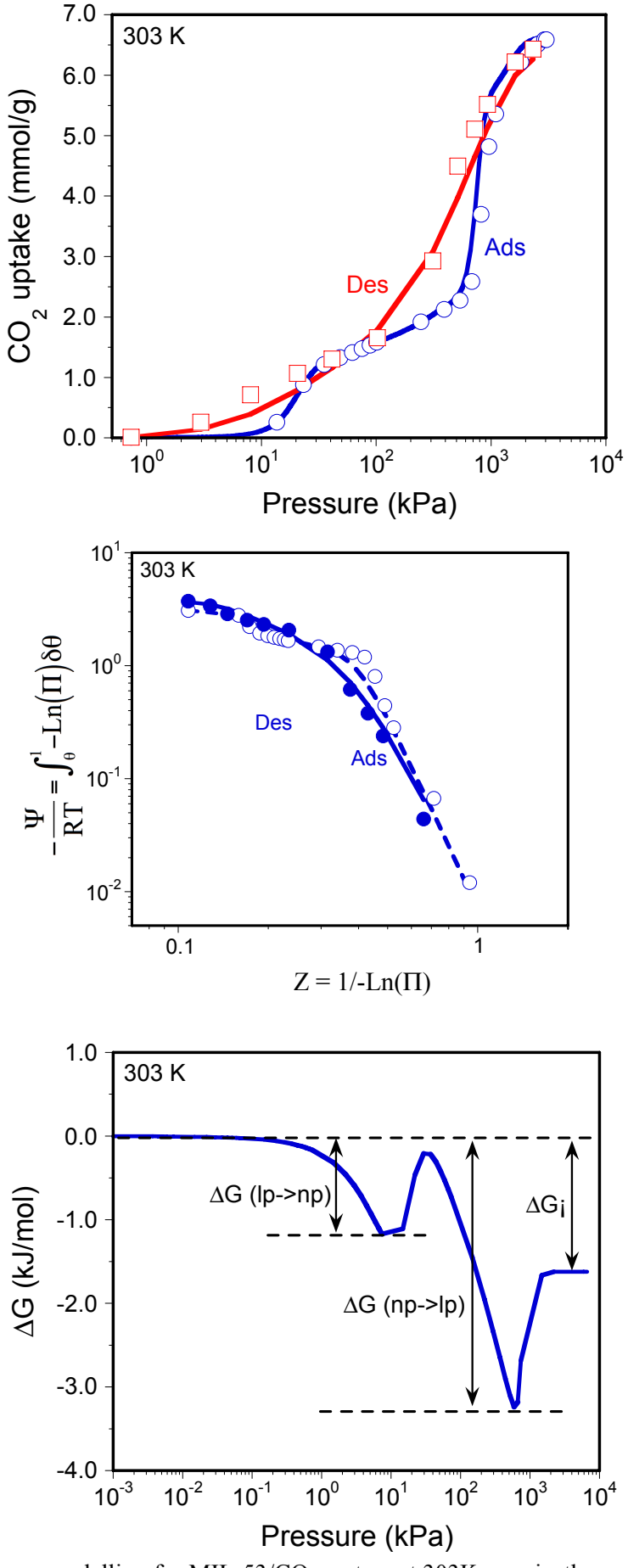

Figure S6: Isotherm modelling for MIL-53/CO_2 system at 303K; raw isotherm; thermodynamic representation; and free energy changes upon adsorption.

Table S6: Adsorption curve

T (K)	*G°*	*First zone*		*Second zone*		*Third zone*		*Fourth zone*	
		m_1	Z_1	m_2	Z_2	m_3	Z_3	m_4	Z_4
303	3.08	24 ± 1	0.173 ± 0.001	1.07 ± 0.03	0.277 ± 0.002	43 ± 20	0.43 ± 0.01	6.0 ± 0.6	0.362 ± 0.01

Table S7: Desorption curve

T (K)	*G°*	*First zone*		*Second zone*		*Third zone*		*Fourth zone*	
		m_1	Z_1	m_2	Z_2	m_3	Z_3	m_4	Z_4
303	3.72	9 ± 2	0.166 ± 0.005	2.0 ± 0.3	0.25 ± 0.01	6 ± 1	0.300 ± 0.03	5.2± 0.3	0.280 ± 0.003

Table S8: Phase transition (data in kJ/mol)

T (K)	*ΔG° (kJ/mol)*	*ΔG_I (des->ads) (kJ/mol)*	*ΔG_I (lp1->np) (kJ/mol)*	*$P_{peak,I}$ (kPa)*	*ΔG_{II} (des->ads) (kJ/mol)*	*ΔG_I (np->lp2) (kJ/mol)*	*$P_{peak,II}$ (kPa)*
303	-1.6	-1.2	-1.1	7.4	-3.2	-2.3	592

5.3- ELM-11 at 273K

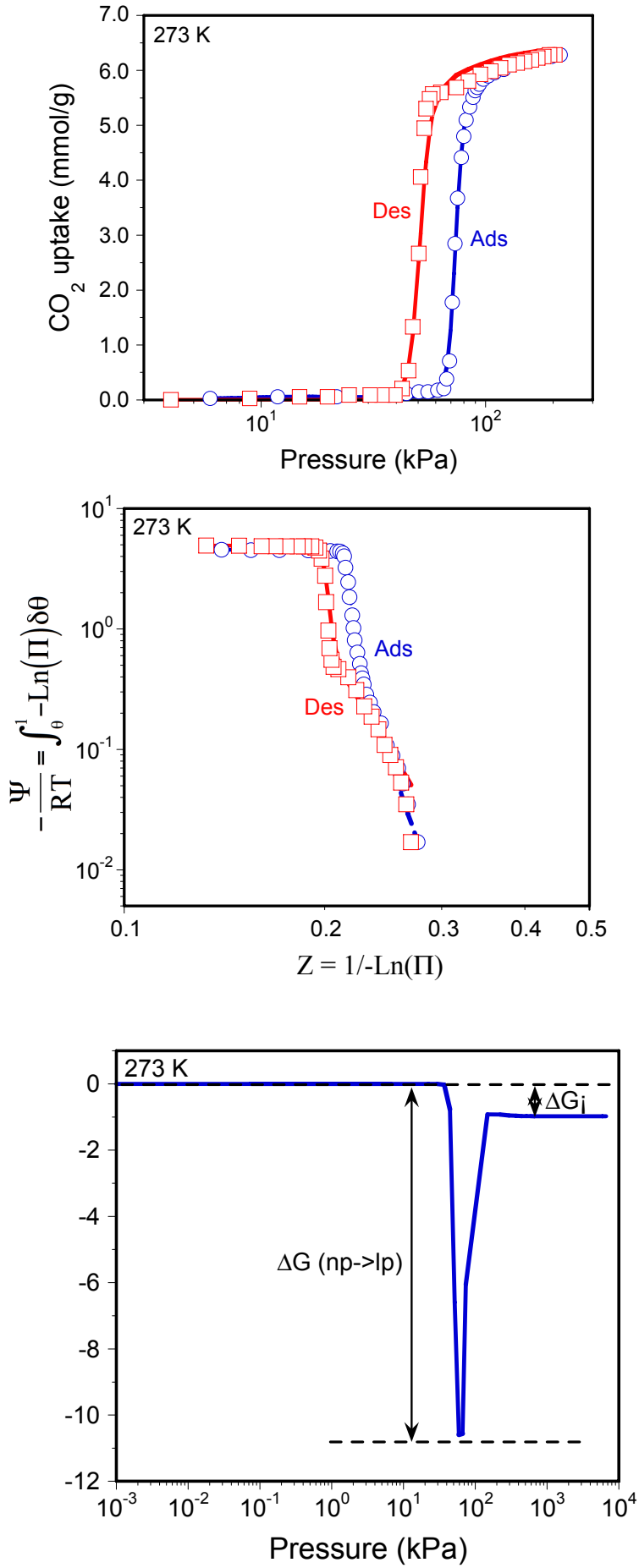

Figure S7: Isotherm modelling for ELM-11/CO_2 system at 273K; raw isotherm; thermodynamic representation; and free energy changes upon adsorption.

Table S9: Adsorption curve

T (K)	*G°*	*First zone*		*Fourth zone*	
		m_1	Z_1	m_4	Z_4
273	4.55	122 ± 5	0.217 ± 0.001	15 ± 3	0.38 ± 0.01

Table S10: Desorption curve

T (K)	*G°*	*First zone*		*Fourth zone*	
		m_1	Z_1	m_4	Z_4
273	4.61	99 ± 8	0.201 ± 0.001	9.3 ± 0.6	0.165 ± 0.003

Table S11: Phase transition (data in kJ/mol)

T (K)	*ΔG° (kJ/mol)*	*ΔG (des->ads) (kJ/mol)*	*ΔG (α->β) (kJ/mol)*	P_{peak} *(kPa)*
273	-1.0	-10.6	-7.6	59.2